Available online at www.sciencedirect.com
SCIENCE DIRECT®
Journal of Molecular Spectroscopy 229 (2005) 257–265
Journal of MOLECULAR SPECTROSCOPY
www.elsevier.com/locate/jms

Infrared and near infrared emission spectra of SbH and SbD

Shanshan Yu[a], Dejian Fu[a], Alireza Shayesteh[a], Iouli E. Gordon[b], Dominique R.T. Appadoo[a], Peter Bernath[a,b,*]

[a] Department of Chemistry, University of Waterloo, Waterloo, Ont., Canada N2L 3G1
[b] Department of Physics, University of Waterloo, Waterloo, Ont., Canada N2L 3G1

Received 13 July 2004; in revised form 13 September 2004

Abstract

The $X^3\Sigma^-$ ground state vibration–rotation spectrum of SbH and the near infrared spectra of the $b^1\Sigma^+$–$X^3\Sigma^-$ transitions of SbH and SbD have been measured at high resolution by Fourier transform spectroscopy. The SbH and SbD radicals were generated in a tube furnace with a D.C. discharge of a flowing mixture of argon, hydrogen (or deuterium), and antimony vapor. In the infrared region, the 1–0 and 2–1 bands of the three components (0^+, 1_e, and 1_f) as well as the 0^+ component of the 3–2 band were observed for ^{121}SbH and ^{123}SbH. In the near infrared region, the 0–0, 1–1, and 2–2 bands of the $b^1\Sigma^+$–$X^3\Sigma^-$ system of both SbH and SbD as well as the 3–3 band of SbD were observed. Except for a few lines, the antimony isotopic shift was not resolved for these electronic spectra. The present data set was combined with the available ground state data on SbD and $a^1\Delta$ data for SbH and SbD from previous work, and a least-squares fit was performed for each of the four isotopologues: ^{121}SbH, ^{123}SbH, ^{121}SbD, and ^{123}SbD. Improved spectroscopic constants were obtained for the observed vibrational levels of the $X^3\Sigma^-$, $a^1\Delta$, and $b^1\Sigma^+$ states of these four isotopologues. In addition, all the above data were also fitted simultaneously to a multi-isotopologue Dunham model, which yielded Dunham constants and Born–Oppenheimer breakdown parameters for these three electronic states. Interestingly, we found that Born–Oppenheimer breakdown corrections were also required for some of the spin–spin and spin–rotation parameters of the $X^3\Sigma^-$ state.

Keywords: SbH; SbD; Infrared spectra; Electronic spectra; Spin–spin; Spin–rotation; Born–Oppenheimer; Dunham

1. Introduction

SbH and SbD radicals are the least studied of the Group V diatomic hydrides. The first observation of SbH and SbD was reported in 1972 by Bollmark and Lindgren [1], and Basco and Yee [2], who independently measured the $A^3\Pi_i$–$X^3\Sigma^-$ absorption spectra by flash photolysis of stibine. Seven years later, Bollmark and Lindgren [3] made new observations of the $A^3\Pi_i$–$X^3\Sigma^-$ transition, which permitted them to perform a detailed rotational analysis and derive molecular constants for the $A^3\Pi_i$ and $X^3\Sigma^-$ states. In 1981, Bollmark et al. [4] studied the absorption spectra of the SbH and SbD in the region 1900–1580 Å by the flash discharge technique and some improvements of the ground state constants were obtained together with information about several new upper states.

More precise molecular constants for the $X^3\Sigma^-$ ground state of SbH were obtained by Stackmann et al. [5], who studied the spectrum of SbH by the infrared laser magnetic resonance technique. Improved spectroscopic constants for the $X^3\Sigma^-$ ground state of SbD were obtained by Urban et al. [6] in their study of the fundamental bands and the 2–1 hot bands of SbH and SbD with a tunable diode laser. Recently, Beutel et al. [7] measured the 0–0 and

* Corresponding author. Fax: +1 519 746 0435.
E-mail address: bernath@uwaterloo.ca (P. Bernath).

0022-2852/$ - see front matter © 2004 Elsevier Inc. All rights reserved.
doi:10.1016/j.jms.2004.09.012

1–1 bands of the $a^1\Delta$–$X^3\Sigma^-$ transitions of SbH and SbD with a Fourier transform spectrometer. Shestakov et al. [8] studied the $b^1\Sigma^+$–$X^3\Sigma^-$ transitions of SbH and SbD by pulsed laser excitation spectroscopy. The spectra of Shestakov et al. [8] directly measured the large spin splitting of about 660 cm^{-1} between the $X_1 0^+$ and $X_2 1$ spin components of the $X^3\Sigma^-$ state. More recently, Wang et al. [9] observed infrared spectra of several antimony hydrides including SbH and SbD in solid matrices. In addition, several theoretical calculations [10–12] were also carried out for SbH and SbD.

Recently, our laboratory has been recording infrared spectra of metal monohydrides (e.g., BeH [13], MgH [14]) and metal dihydrides (e.g., BeH_2 [15], MgH_2 [16]). Our interest in SbH was sparked by the fact that the ro-vibrational data for SbH were very sparse, and the possibility of observing the SbH_2 radicals. The number of infrared lines for SbH was roughly six times less than that for SbD in the experiments of Urban et al. [6]. They did not have a suitable laser diode for SbH and thus only observed eight lines (none of which turned out to be correct) for the infrared bands of the $X_1 0^+$ spin component. They also measured a number of lines from the weaker $X_2 1$ spin component, which turned out to be correct.

2. Experiment

SbH and SbD were generated in a D.C. discharge (2.8 kV, 333 mA) of a flowing mixture of 2 Torr of hydrogen or deuterium and 2.5 Torr argon in an alumina tube (5 cm × 120 cm), which contained antimony metal powder (10 g) heated to 800 °C. The emitted radiation was focused by a CaF_2 lens into the entrance aperture of a Bruker IFS 120 HR Fourier transform spectrometer.

Electronic spectra of the SbH and SbD radicals were measured at a resolution of 0.05 cm^{-1} in the 8000–15 000 cm^{-1} region with a visible quartz beamsplitter and a silicon diode detector. The spectrometer was not evacuated so that the "air" wavenumbers of the lines were first corrected to vacuum wavenumbers [17] and then calibrated to the argon atomic lines [18] that appear in the spectra. The precision of the measured wavenumbers is approximately 0.003 cm^{-1} for the lines from the 1_f component but 0.01 cm^{-1} for the lines from the 0^+ and 1_e components due to the overlapping of lines from ^{121}SbH and ^{123}SbH. Antimony has two isotopes ^{121}Sb and ^{123}Sb with natural abundances of 57.3 and 42.7%, respectively.

An infrared spectrum of SbH was recorded in the 1200–2200 cm^{-1} region at a resolution of 0.01 cm^{-1} with

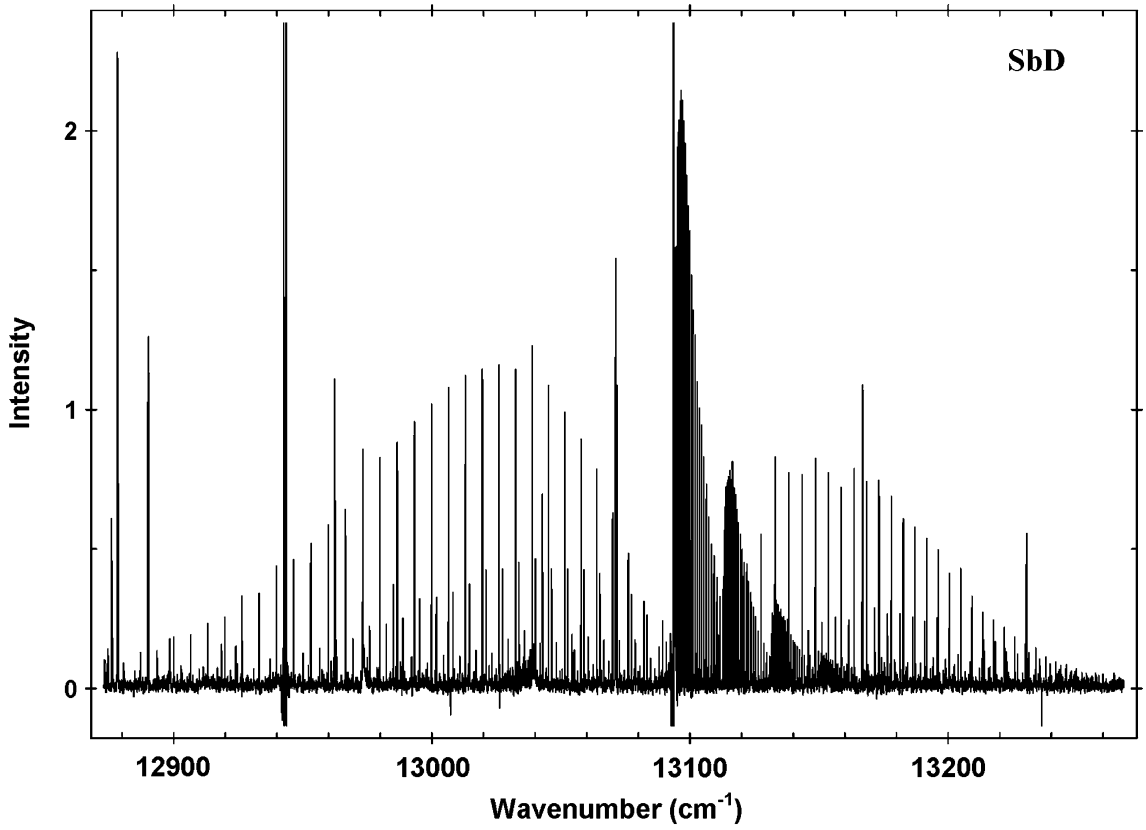

Fig. 1. An overview spectrum of the $b^1\Sigma^+$–$X_2 1$ transition of SbD recorded at a resolution of 0.05 cm^{-1}. The atomic lines are from argon, and they were used to calibrate the spectrum.

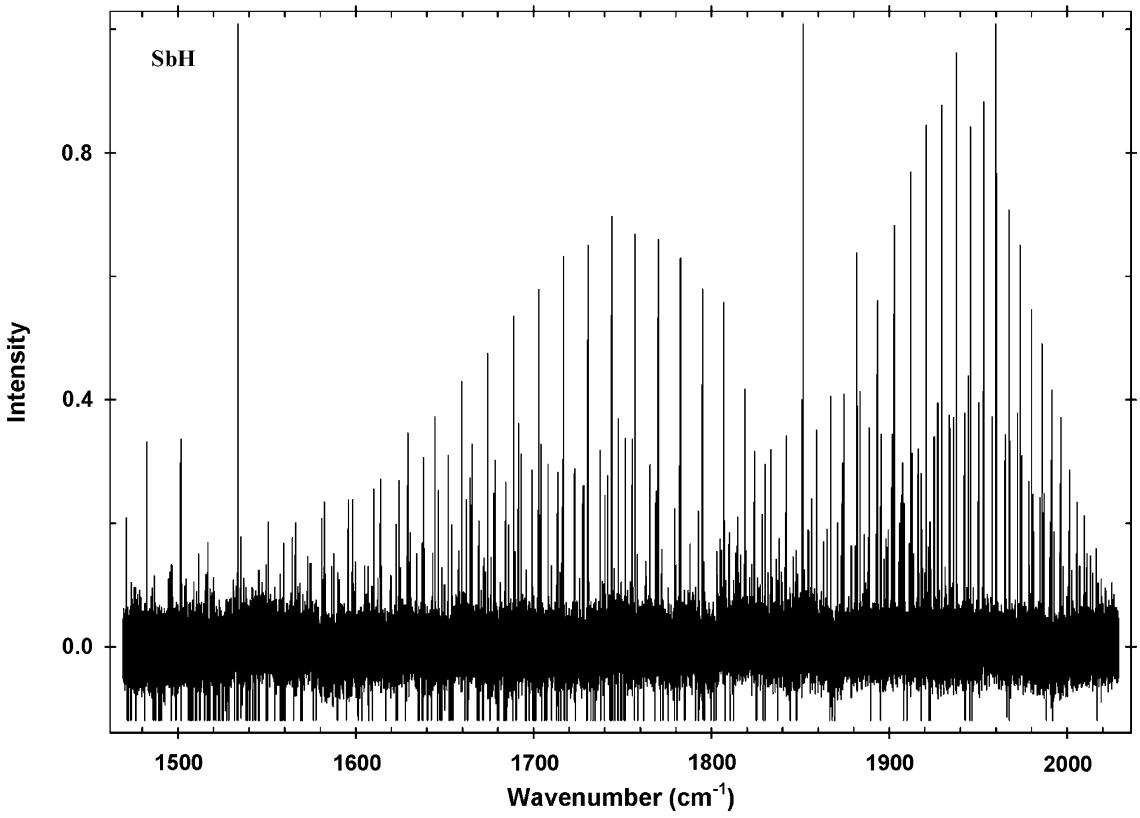

Fig. 2. An overview of the $X^3\Sigma^-$ ground state infrared spectrum of SbH recorded at a resolution of 0.01 cm^{-1}. The baseline was corrected with the Bruker OPUS software and the absorption lines are due to atmospheric H_2O vapor.

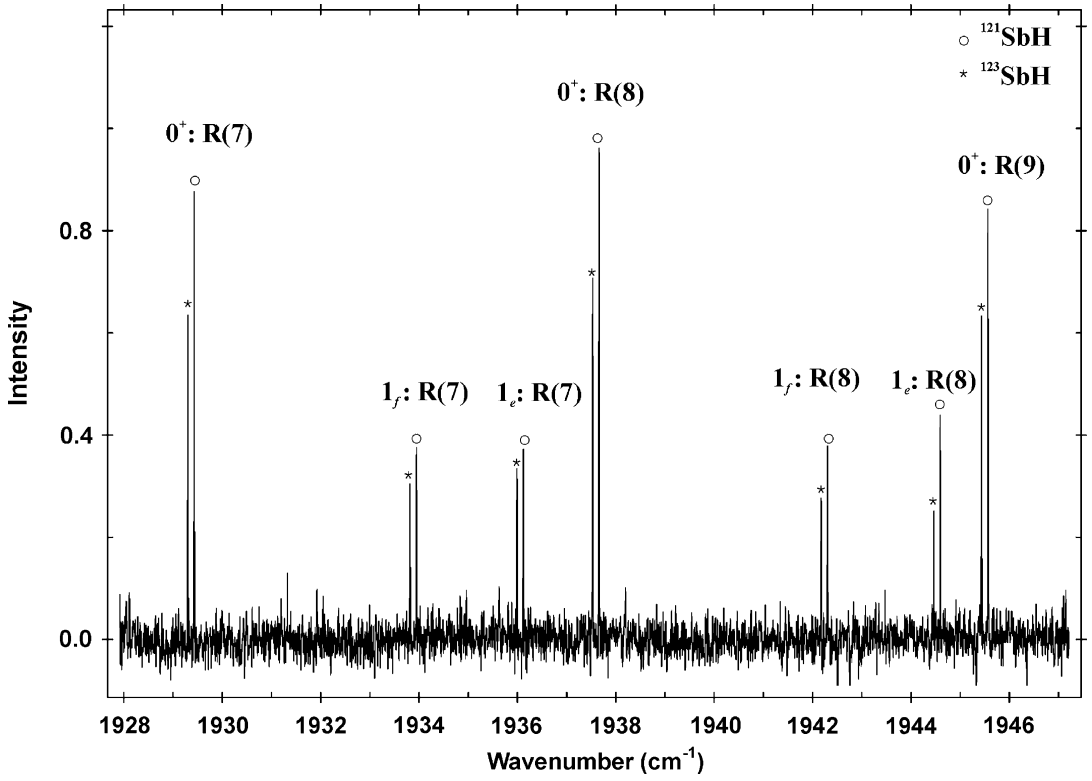

Fig. 3. An expanded view of the R branch of the 1–0 band of the $X^3\Sigma^-$ state of SbH near 1930 cm^{-1}. The lines are doubled due to the ^{121}Sb and ^{123}Sb isotopes. The doublets of the 1_e and 1_f components have about 50% of the intensity of the 0^+ component.

a KBr beamsplitter and a liquid nitrogen-cooled HgCdTe (MCT) detector. This SbH spectrum was calibrated by use of 13 SbH lines measured by Urban et al. [6] by diode laser spectrometer. (Although their lines positions of the 0^+ component were not correct, these 13 lines from the 1_e and 1_f components proved to be correct.) Our SbH lines in the infrared region should have an absolute accuracy of about $0.001\ cm^{-1}$. A much weaker SbD spectrum was also measured at a resolution of $0.01\ cm^{-1}$ in the $800–2500\ cm^{-1}$ region, but was not used in our analysis because of the low signal-to-noise ratio. Instead the extensive diode laser data of Urban et al. [6] for SbD were used in our analysis.

3. Results and discussion

In the near infrared spectra of both SbH and SbD, five branches, ^{S}R, ^{Q}P, $^{Q}Q_{ef}$, ^{Q}R, and ^{O}P, were observed for the 0–0, 1–1, and 2–2 bands of the $b^1\Sigma^+–X^3\Sigma^-$ transition. In addition, the 3–3 band of SbD was also observed. Fig. 1 shows the spectrum of the $b^1\Sigma^+–X_21$ transition of SbD that we obtained. Our line positions agree well with those reported by Shestakov et al. [8] within their error limits.

In the infrared region (Fig. 2), we observed the fundamental band and the 2–1 hot band for the 0^+, 1_e, and 1_f spin components and the 3–2 hot band of the 0^+ component for both ^{121}SbH and ^{123}SbH. Our line positions for the 0^+ component differ substantially from those reported by Urban et al. [6], with the largest difference being $1.9\ cm^{-1}$. However, our line positions for the 1_e and 1_f components agree very well with their data. We also observed the fundamental band of SbD but with a relatively low signal-to-noise ratio. In this case, our line positions of all three components agreed very well with those reported by Urban et al. [6]. Therefore, we believe that the line positions of the 1_e and 1_f components of SbH of Urban et al. [6] are reliable and used these lines for the absolute wavenumber calibration of our SbH spectrum Fig. 3.

Antimony has two isotopes ^{121}Sb and ^{123}Sb so the infrared lines appear as doublets with a relative intensity of 4:3 [6,8]. The transitions of the 1_e and 1_f components have about 50% of the intensity of the 0^+ component. Since we only observed the $\Delta v = 0$ sequence of the $b^1\Sigma^+–X^3\Sigma^-$ system of SbH and SbD, the isotopic splitting due to the antimony atom was only observed at high J values ($J > 25$) of the 0^+ and 1_e components of the $b^1\Sigma^+–X^3\Sigma^-$ transition.

We performed a least-squares fit for each of the four isotopologues: ^{121}SbH, ^{123}SbH, ^{121}SbD, and ^{123}SbD. The data sets for ^{121}SbH and ^{123}SbH included the $X^3\Sigma^-$ ground state infrared data (both our FTS and the diode laser lines [6]), the $b^1\Sigma^+–X^3\Sigma^-$ transition observed in our experiment, and the $a^1\Delta–X^3\Sigma^-$ lines reported by Beutel et al. [7].

Table 1
Spectroscopic constants (in cm^{-1}) for the $X^3\Sigma^-$, $a^1\Delta$ and $b^1\Sigma^+$ states of ^{121}SbH and ^{123}SbH (all uncertainties are 1σ)[a]

State	Constants	$v = 0$		$v = 1$		$v = 2$		$v = 3$	
		^{121}SbH	^{123}SbH	^{121}SbH	^{123}SbH	^{121}SbH	^{123}SbH	^{121}SbH	^{123}SbH
$X^3\Sigma^-$	T_v	0	0	1854.17310(18)	1854.05355(22)	3640.07809(32)	3639.84809(40)	5357.20432(88)	5356.87143(99)
	B_v	5.6830941(74)	5.6823780(91)	5.5257362(67)	5.5250442(86)	5.3676276(76)	5.366966(12)	5.2060522(99)	5.205426(12)
	10^4D_v	2.06289(31)	2.06362(36)	2.05652(27)	2.05695(35)	2.05484(30)	2.05546(65)	2.01139(29)	2.01249(34)
	10^9H_v	3.052(39)	3.217(43)	2.937(31)	3.057 (41)	2.736(36)	2.92(12)	—	—
	γ_v	−0.23922(15)	−0.23994(18)	−0.19332(15)	−0.19402(18)	−0.14481(18)	−0.14535(21)	−0.09368[b]	−0.09386[b]
	$10^5\gamma_{D_v}$	7.037(28)	7.152(32)	8.147(27)	8.259(30)	9.441(43)	9.555(46)	—	—
	λ_v	333.33269(48)	333.33439(54)	334.27953(47)	334.28153(53)	335.00807(49)	335.01012(55)	335.51822[b]	335.52028[b]
	$10^3\lambda_{D_v}$	1.9492(24)	1.9567(29)	1.7868(24)	1.7927(29)	1.5112(26)	1.5201(31)		
$a^1\Delta$	T_v	6380.7823(26)	6380.7819(30)	8256.9333(98)	8256.809(11)				
	B_v	5.706694(69)	5.706032(76)	5.55268(51)	5.55259(61)				
	10^4D_v	2.0388(37)	2.0387(39)	2.021(57)	2.075(72)				
$b^1\Sigma^+$	T_v	13321.15387(78)	13321.15427(91)	15202.3132(10)	15202.1937(12)	17014.4636(16)	17014.2371(21)		
	B_v	5.717920(11)	5.717218(13)	5.561834(16)	5.561165(19)	5.404247(39)	5.403503(44)		
	10^4D_v	2.04249(36)	2.04336(42)	2.03773(61)	2.03855(73)	2.0489(23)	2.0438(24)		
	10^9H_v	3.019(41)	3.191(45)	2.697(62)	2.834(75)	3.42(39)	2.63(38)		

[a] Fitted to the $X^3\Sigma^-$ ground state infrared data (both our FTS and the diode laser lines [6]), the $b^1\Sigma^+–X^3\Sigma^-$ lines observed in our experiment, and the $a^1\Delta–X^3\Sigma^-$ lines reported by Beutel et al. [7].
[b] Fixed values determined by extrapolation of the corresponding constants for $v = 0–2$.

ported by Beutel et al. [7]. For ^{121}SbD and ^{123}SbD, the data sets included the $X^3\Sigma^-$ ground state infrared data reported by Urban et al. [6], the $b^1\Sigma^+$–$X^3\Sigma^-$ transition observed in our work, and the $a^1\Delta$–$X^3\Sigma^-$ transition reported by Beutel et al. [7]. In these fits, the data for the $b^1\Sigma^+$–$X\,^3\Sigma^-$ and $a^1\Delta$–$X^3\Sigma^-$ transitions were almost identical for the ^{121}SbH/^{123}SbH and ^{121}SbD/^{123}SbD pairs except for a few high J lines with resolved Sb isotopic splitting. Because there are no infrared bands to connect with the 3–3 band of the $b^1\Sigma^+$–$X^3\Sigma^-$ transition of SbD, this band was fitted separately.

The energy levels of both the $b\ ^1\Sigma^+$ and $a^1\Delta$ states were represented by the standard formula [19]

$$F(J) = T_v + B_v J(J+1) - D_v[J(J+1)]^2 + H_v[J(J+1)]^3. \quad (1)$$

The energy levels of the $X^3\Sigma^-$ ground state were calculated by use of the usual Hamiltonian matrix with matrix elements derived with Hund's case (a) basis functions [20]. The obtained spectroscopic constants of the $X^3\Sigma^-$, $b^1\Sigma^+$, and $a\ ^1\Delta$ states for SbH are given in Table 1 and the corresponding constants for SbD are in Table 2. The spectroscopic constants for the 3–3 band of SbD are given separately in Table 3. Since only the transitions of the 0^+ component of the 3–2 band were observed for ^{121}SbH and ^{123}SbH in our infrared spectrum, the spin–spin constant, λ_3'', and the spin–rotation constant, γ_3'', of the $X^3\Sigma^-$ state were fixed to estimated values determined by extrapolation in the fits of these two isotopes. An estimated value was also used for the spin–rotation constant, γ_3'', in the separate fit of 3–3 band of the $b^1\Sigma^+$–$X^3\Sigma^-$ transition of SbD. The output files of our fits are provided in the supplementary tables S1–S5: Table S1 for ^{121}SbH, Table S2 for ^{123}SbH, Table S3 for ^{121}SbD, Table S4 for ^{123}SbD, and Table S5 for the separate fit of 3–3 band of the $b^1\Sigma^+$–$X^3\Sigma^-$ transition of SbD.

In the initial stages of our fits, we used the same data for the $b^1\Sigma^+$–$X^3\Sigma^-$ transition for the ^{121}SbH/^{123}SbH and ^{121}SbD/^{123}SbD pairs. A systematic trend in the observed minus calculated line positions was found for nearly all of the bands of the $b^1\Sigma^+$–$X^3\Sigma^-$ transition. The residuals were positive in the P branches and negative in the R branches of ^{121}SbH and ^{121}SbD. For ^{123}SbH and ^{123}SbD the signs of the residuals changed and they were negative in the P branches and positive in the R branches. The residuals also increased with increasing J values. It was found that the unresolved lines of the two antimony isotopes cause these systematic trends. After we added the resolved high-J lines, the trend in the residuals of these few lines disappeared

Table 3
Spectroscopic constants (in cm^{-1}) for the $X^3\Sigma^-$ and $b^1\Sigma^+$ states of SbD ($v = 3$) from the separate fit of the 3–3 band. (all uncertainties are 1σ)

State	Constants	Value
$X^3\Sigma^-$	B_3	2.71047(16)
	$10^4\ D_3$	0.5566(30)
	γ_3	−0.02001[a]
	λ_3	334.8411(26)
	$10^3\lambda_{D_3}$	0.857(15)
$b^1\Sigma^+$	T_{3-3}	13372.8154(30)[b]
	B_3	2.72941(15)
	$10^4\ D_3$	0.5535(29)

[a] Fixed value determined by extrapolation of γ_v from $v = 0$–2.
[b] Band origin of the 3–3 band of the $b^1\Sigma^+$–$X^3\Sigma^-$ transition of SbD.

Table 2
Spectroscopic constants (in cm^{-1}) for the $X^3\Sigma^-$, $a^1\Delta$ and $b^1\Sigma^+$ states of ^{121}SbD and ^{123}SbD (all uncertainties are 1σ)[a]

State	Constants	$v = 0$		$v = 1$		$v = 2$	
		^{121}SbD	^{123}SbD	^{121}SbD	^{123}SbD	^{121}SbD	^{123}SbD
$X^3\Sigma^-$	T_v	0	0	1331.25546(21)	1331.08415(20)	2628.1647(22)	2627.8277(23)
	B_v	2.879930(10)	2.8792906(81)	2.8235738(94)	2.8229452(76)	2.767072(15)	2.766440(16)
	10^4D_v	0.52488(21)	0.52673(17)	0.52362(19)	0.52525(16)	0.52305(24)	0.52362(24)
	10^9H_v	0.307(13)	0.454(10)	0.308(11)	0.4372(86)	0.348(12)	0.4316(90)
	γ_v	−0.11328(23)	−0.11377(26)	−0.08506(22)	−0.08504(25)	−0.05401(65)	−0.05466(73)
	$10^5\gamma_{D_v}$	1.769(25)	1.892(24)	2.384(23)	2.435(23)	3.111(85)	2.772(97)
	λ_v	333.02596(57)	333.02534(59)	333.73637(56)	333.73606(58)	334.35316(99)	334.3533(11)
	$10^3\lambda_{D_v}$	0.9819(15)	0.9802(17)	0.9328(15)	0.9315(16)	0.8570(40)	0.8435(56)
$a^1\Delta$	T_v	6389.1503(25)	6389.1476(27)	7735.3033(54)	7735.1280(51)		
	B_v	2.891087(33)	2.890490(33)	2.836074(75)	2.835590(72)		
	10^4D_v	0.51584(80)	0.51794(79)	0.5185(20)	0.5237(20)		
$b^1\Sigma^+$	T_v	13316.09396(87)	13316.09281(90)	14666.56238(82)	14666.39038(88)	15982.4632(23)	15982.1259(25)
	B_v	2.897829(11)	2.897195(10)	2.842011(11)	2.8413851(95)	2.785864(19)	2.785247(20)
	10^4D_v	0.51967(22)	0.52163(20)	0.51897(20)	0.52066(18)	0.51893(44)	0.52017(49)
	10^9H_v	0.298(14)	0.450(11)	0.305(12)	0.4369(94)	0.309(32)	0.449(34)

[a] Fitted to the $X^3\Sigma^-$ state infrared data reported by Urban et al. [6], the $b^1\Sigma^+$–$X^3\Sigma^-$ transition observed in our experiment, and the $a^1\Delta$–$X^3\Sigma^-$ transition reported by Beutel et al. [7].

while the systematic trend remained for the unresolved low J lines. Ultimately some of these low J lines were simply deweighted in our final fits.

Table 4 shows a comparison of the spectroscopic constants for $v = 0$ with the recent literature values. The new constants have a higher precision and are more extensive than the previous work. They agree reasonably well with the constants of Fink and coworkers [7,8], but less well with those of Urban et al. [6]. In fact it is a surprise that the constants of SbH reported by Urban et al. [6] are even in modest agreement with our results because their line positions for the 0^+ component differ substantially from our measurements.

All lines of four isotopologues of SbH were also fitted simultaneously to a multi-isotopologue Dunham model [21] using DPARFIT [22], a FORTRAN code written originally to fit closed-shell electronic states of diatomic molecules. This code has been altered and, presently, can perform fits to transitions belonging to $^2\Sigma$ as well as $^3\Sigma$ electronic states.

The Hund's coupling case (a) matrix elements for $^3\Sigma$ state [20], which were also used in our least-squares fits to generate the constants of Tables 1 and 2, were coded in DPARFIT to analyze the ground $X^3\Sigma^-$ state of SbH. These matrix elements are listed for convenience in Table 5 in the form of multiplicative factors. In DPARFIT, the parameters representing the ro-vibrational (G_v, B_v, $-D_v$ and H_v), the spin–rotation (γ_v), and spin–spin (λ_v) interactions in Table 5 were expressed using the following Dunham-type vibrational expansions:

$$\begin{aligned} G_v &= \sum_{l=1} Y_{l,0}\left(v+\frac{1}{2}\right)^l, \quad B_v = \sum_{l=0} Y_{l,1}\left(v+\frac{1}{2}\right)^l, \\ -D_v &= \sum_{l=0} Y_{l,2}\left(v+\frac{1}{2}\right)^l, \quad H_v = \sum_{l=0} Y_{l,3}\left(v+\frac{1}{2}\right)^l; \end{aligned} \tag{2}$$

$$\begin{aligned} \gamma_v &= \sum_{l=0} \gamma_{l,0}\left(v+\frac{1}{2}\right)^l, \quad \gamma_{Dv} = \sum_{l=0} \gamma_{l,1}\left(v+\frac{1}{2}\right)^l, \\ \gamma_{Hv} &= \sum_{l=0} \gamma_{l,2}\left(v+\frac{1}{2}\right)^l; \end{aligned} \tag{3}$$

$$\lambda_v = \sum_{l=0} \lambda_{l,0}\left(v+\frac{1}{2}\right)^l, \quad \lambda_{Dv} = \sum_{l=0} \lambda_{l,1}\left(v+\frac{1}{2}\right)^l. \tag{4}$$

For the 1_f component, a simple energy level expression (see Table 5) given by

$$E(v,J) = H_{11}^f \tag{5}$$

was used. For the 0^+ and 1_e energy levels, a 2×2 matrix was diagonalized analytically (see Table 5) using the formula

Table 4
A comparison of spectroscopic constants (in cm^{-1}) for the $X^3\Sigma^-$, $a^1\Delta$ and $b^1\Sigma^+$ states of SbH and SbD ($v = 0$)

State	Constants	^{121}SbH				^{121}SbD			
		Present work	Shestakov et al.[a]	Urban et al.[b]	Beutel et al.[c]	Present work	Shestakov et al.[a]	Urban et al.[b]	Beutel et al.[c]
$X^3\Sigma^-$	B_0	5.6830941(74)	5.6825(3)	5.684417(85)		2.879930(10)	2.8798(1)	2.880600(19)	
	$10^4 D_0$	2.06289(31)	2.05(1)	2.1095(99)		0.52488(21)	0.528(7)	0.52574(31)	
	$10^9 H_0$	3.052(39)	—	2.921		0.307(13)	—	0.375(24)	
	γ_0	−0.23922(15)	−0.238(6)	−0.2319(17)		−0.11328(23)	−0.117(3)	−0.11086(14)	
	$10^5\gamma_{D_0}$	7.037(28)	6(3)	8.5(15)		1.769(25)	3.1(9)	1.53(19)	
	λ_0	333.33269(48)	333.373(4)	333.29758(53)		333.02596(57)	333.0884(7)	333.36984(20)	
	$10^3\lambda_{D_0}$	1.9492(24)	2(1)	1.044(47)		0.9819(15)	0.94(4)	1.007(18)	
$a^1\Delta$	T_0	6380.7823(26)			[6175.349(2)][d]	6389.1503(25)			[6175.6705(5)][d]
	B_0	5.706694(69)			5.70465(8)	2.891087(33)			2.89033(3)
	$10^4 D_0$	2.0388(37)			2.041(4)	0.51584(80)			0.5163(6)
$b^1\Sigma^+$	T_0	13321.15387(78)	[13098.623(4)][e]			13316.09396(87)	[13093.844(6)][e]		
	B_0	5.717920(11)	5.7175(3)			2.897829(11)	2.8976(2)		
	$10^4 D_0$	2.04249(36)	2.04(1)			0.51967(22)	0.519(6)		
	$10^9 H_0$	3.019(41)	—			0.298(14)	—		

[a] Constants derived from unresolved lines of ^{121}SbH and ^{123}SbH from [8].
[b] Constants calculated by use of the equilibrium constants for ^{121}SbH from [6].
[c] Constants derived from unresolved lines of ^{121}SbH and ^{123}SbH from [7].
[d] Band origins of the 0–0 band of the $b^1\Sigma^+$–$X_2 1$ transition from [7], which can not be directly compared with our constants.
[e] Band origins of the 0–0 band from [8], which can not be directly compared with our constants.

Table 5
Coefficients and multiplicative factors of the matrix elements of $^3\Sigma$ state

Constants	(H^e_{11})[a]	(H^e_{12})[a]	(H^e_{22})[a]	(H^f_{11})[b]
G_v	1	0	1	1
B_v	$(2+x)$[c]	$-2x^{1/2}$	x	x
D_v	$-(4+8x+x^2)$	$2x^{1/2}\,(2+2x)$	$-(4x+x^2)$	$-x^2$
H_v	$(8+28x+18x^2+x^3)$	$-2x^{1/2}\,(4+10x+3x^2)$	$(8x+12x^2+x^3)$	x^3
γ_v	-2	$x^{1/2}$	-1	-1
γ_{D_v}	$-2(2+2x)$	$x^{1/2}\,(4+x)$	$-3x$	$-x$
γ_{H_v}	$-2(4+10x+3x^2)$	$x^{1/2}\,(8+12x+x^2)$	$-(8x+5x^2)$	$-x^2$
λ_v	$-4/3$	0	2/3	2/3
λ_{D_v}	$-(4/3)(2+x)$	$(2/3)\,x^{1/2}$	$(2/3)x$	$(2/3)x$

[a] Matrix elements for the 2×2 matrix for the $0^+(e)$ and 1_e components.
[b] Matrix element for the 1_f component.
[c] $x = J(J+1)$.

$$E(v,J) = \frac{1}{2}\left[(H^e_{11}+H^e_{22}) \pm \sqrt{(H^e_{11}-H^e_{22})^2+4(H^e_{12})^2}\right] \quad (6)$$

to obtain the energy levels, with the 1_e levels lying above the 0^+ levels for the same value of J.

Once individual Dunham-type fits for each isotopologue were completed, a combined fit was carried out

Table 6
Dunham and Born–Oppenheimer breakdown constants (in cm^{-1}) for the $X^3\Sigma^-$ state of ^{121}SbH, ^{123}SbH, ^{121}SbD, and ^{123}SbD

	^{121}SbH	^{123}SbH	^{121}SbD	^{123}SbD
$Y_{1,0}$	1921.8348(28)	1921.705503(2800)	1365.482901(5000)	1365.300805(5000)
$Y_{2,0}$	−33.65907(220)	−33.654541(2200)	−17.078058(3700)	−17.073503(3700)
$Y_{3,0}$	−0.10556(48)	−0.1055387(4800)	−0.0217142(8000)	−0.0217055(8000)
$Y_{0,1}$	5.761538(16)	5.76076278(1600)	2.90808829(960)	2.90731272(960)
$Y_{1,1}$	−0.1566201(91)	−0.15658849(910)	−0.05621976(420)	−0.05619727(420)
$10^4 Y_{2,1}$	−3.734(32)	−3.733(32)	−0.705(14)	−0.70462(1400)
$10^4 Y_{0,2}$	−2.06852(65)	−2.0679634(6500)	−0.5265107(1700)	−0.5262299(1700)
$10^7 Y_{1,2}$	8.10(44)	8.0973(4400)	1.46443(8000)	1.46346(8000)
$10^8 Y_{2,2}$	4.0(32)	3.998(3200)	0.5137(4100)	0.5133(4000)
$10^8 Y_{3,2}$	−6.50(74)	−6.4969(7400)	−0.59289(6700)	−0.59233(6700)
$10^9 Y_{0,3}$	3.330(86)	3.32866(8600)	0.42763(1100)	0.42729(1100)
$10^{10} Y_{1,3}$	−1.80(31)	−1.7992(3100)	−0.16418(2800)	−0.16403(2800)
$\gamma_{0,0}$	−0.25620(41)	−0.256166(410)	−0.126232(200)	−0.126198(200)
$10^2\gamma_{1,0}$	2.628(59)	2.62747(5900)	2.28991(2100)	2.289(21)
$10^2\gamma_{2,0}$	1.4572(400)	1.45681(4000)	0.370908(10000)	0.370711(10000)
$10^3\gamma_{3,0}$	−2.930(80)	−2.929(80)	−0.52973(1400)	−0.52937(1400)
$10^5\gamma_{0,1}$	6.36(15)	6.3583(1500)	1.568(37)	1.5671(370)
$10^6\gamma_{1,1}$	9.10(72)	9.097(720)	5.3938(1300)	5.3902(1300)
$10^7\gamma_{2,1}$	9.0(30)	9.0(30)	1.156(390)	1.155(380)
$10^9\gamma_{0,2}$	4.0(17)	4.0(17)	0.514(210)	0.513(210)
$\lambda_{0,0}$	332.7998(11)	332.7998(11)	332.64092(110)	332.64092(110)
$\lambda_{1,0}$	1.10599(170)	1.105916(1700)	0.785576(1200)	0.785471(1200)
$10^2\lambda_{2,0}$	−6.225(140)	−6.2242(1400)	−3.1406(710)	−3.13977(7100)
$10^2\lambda_{3,0}$	−1.050(33)	−1.04979(3300)	−0.37627(1200)	−0.37612(1200)
$10^3\lambda_{0,1}$	1.9750(38)	1.97473(380)	0.99642(190)	0.99615(190)
$10^5\lambda_{1,1}$	−6.10(28)	−6.099(280)	−2.186(100)	−2.1851(1000)
$10^5\lambda_{2,1}$	−5.26(12)	−5.2586(1200)	−1.3389(300)	−1.3381(300)
$\delta^H_{1,0}$	1.1812(140)			
$\delta^H_{2,0}$	−0.3831(150)			
$10^2\delta^H_{3,0}$	9.00(44)			
$10^3\delta^H_{0,1}$	5.190(25)			
$10^4\delta^H_{1,1}$	−5.28(18)			
$10^4\delta^H_{2,1}$	1.930(94)			
$10^2\delta^{\gamma,H}_{0,0}$	1.20(13)			
$10^2\delta^{\gamma,H}_{1,0}$	7.530(57)			
$10^6\delta^{\gamma,H}_{0,1}$	−4.0(29)			
$10^5\delta^{\gamma,H}_{1,1}$	4.15(13)			
$\delta^{\lambda,H}_{0,0}$	−0.3180(22)			

Table 7
Dunham and Born–Oppenheimer breakdown constants (in cm^{-1}) for the $b^1\Sigma^+$ and $a^1\Delta$ states of ^{121}SbH, ^{123}SbH, ^{121}SbD, and ^{123}SbD

State	Constants	^{121}SbH	^{123}SbH	^{121}SbD	^{123}SbD
$b^1\Sigma^+$	T_e	13307.5411(43)	13307.5411(43)	13306.4964(50)	13306.4964(50)
	$Y_{1,0}$	1949.0838(120)	1948.95267(1200)	1384.64701(860)	1384.46236(860)
	$Y_{2,0}$	−33.6607(100)	−33.656171(10000)	−16.982315(5100)	−16.977786(5100)
	$Y_{3,0}$	−0.1860(24)	−0.185962(2400)	−0.0666536(8800)	−0.0666269(8800)
	$Y_{0,1}$	5.795290(27)	5.79451023(2700)	2.92558879(1500)	2.92480855(1500)
	$Y_{1,1}$	−0.154170(35)	−0.15413889(3500)	−0.05538509(1400)	−0.05536293(1400)
	$10^4 Y_{2,1}$	−9.27(12)	−9.2675(1200)	−1.9907(410)	−1.9897(410)
	$10^4 Y_{0,2}$	−2.04530(67)	−2.0447496(6700)	−0.5206004(1700)	−0.5203228(1700)
	$10^7 Y_{1,2}$	1.80(24)	1.7994(2400)	0.3254(440)	0.3252(440)
	$10^9 Y_{0,3}$	3.220(78)	3.2187(780)	0.4135(100)	0.41317(1000)
	$\delta^H_{1,0}$	0.6440(41)			
	$10^3 \delta^H_{0,1}$	7.063(40)			
	$10^4 \delta^H_{1,1}$	−7.70(67)			
	$10^4 \delta^H_{2,1}$	2.90(31)			
$a^1\Delta$	T_e	6370.5110(97)	6370.5110(97)	6382.0771(108)	6382.0771(108)
	$Y_{1,0}$	1941.989(24)	1941.85835(2400)	1379.37909(1700)	1379.19514(1700)
	$Y_{2,0}$	−32.920(12)	−32.91557(1200)	−16.60862(630)	−16.60419(630)
	$Y_{0,1}$	5.78359(11)	5.7828118(1100)	2.9187627(600)	2.9179842(600)
	$Y_{1,1}$	−0.15378(10)	−0.153749(100)	−0.0551075(360)	−0.0550854(360)
	$10^4 Y_{0,2}$	−2.0370(43)	−2.03645(430)	−0.518488(1100)	−0.518211(1100)
	$10^3 \delta^H_{1,0}$	3.40(10)			

by including corrections for the breakdown of the Born–Oppenheimer approximation. The following expressions were used for the vibration–rotation, spin–spin, and spin–rotation constants:

$$Y^{(\alpha)}_{l,m} = \left\{ Y^{(1)}_{l,m} + \frac{M^{(\alpha)}_H - M^{(1)}_H}{M^{(\alpha)}_H} \delta^H_{l,m} \right\} \left(\frac{\mu_1}{\mu_\alpha} \right)^{m+\frac{l}{2}}, \quad (7)$$

$$\lambda^{(\alpha)}_{l,m} = \left\{ \lambda^{(1)}_{l,m} + \frac{M^{(\alpha)}_H - M^{(1)}_H}{M^{(\alpha)}_H} \delta^{\lambda,H}_{l,m} \right\} \left(\frac{\mu_1}{\mu_\alpha} \right)^{m+\frac{l}{2}}, \quad (8)$$

$$\gamma^{(\alpha)}_{l,m} = \left\{ \gamma^{(1)}_{l,m} + \frac{M^{(\alpha)}_H - M^{(1)}_H}{M^{(\alpha)}_H} \delta^{\gamma,H}_{l,m} \right\} \left(\frac{\mu_1}{\mu_\alpha} \right)^{1+m+\frac{l}{2}}, \quad (9)$$

In Eqs. (7)–(9), the superscript "(1)" is an index for the reference isotopologue chosen to be ^{121}SbH, and the superscript "(α)" is the index for the isotopologue of interest [21]. $M^{(1)}_H$ is the mass of the H atom for the reference isotopologue ^{121}SbH and $M^{(\alpha)}_H$ is the mass of the H/D atom in isotopologue α. The constant μ_1 is the reduced mass of the reference isotopologue ^{121}SbH and μ_α is the reduced mass of isotopologue α. The parameters $\delta^H_{l,m}$, $\delta^{\lambda,H}_{l,m}$, and $\delta^{\gamma,H}_{l,m}$ are coefficients which account for the effect of Born–Oppenheimer breakdown associated with substitution of the H atom by deuterium for the parameters $Y_{l,m}$, $\lambda_{l,m}$, and $\gamma_{l,m}$, respectively. No Born–Oppenheimer breakdown corrections for the Sb atom were needed and the usual mass scaling of Eqs. (7)–(9) was satisfactory.

In the initial fits, Born–Oppenheimer breakdown corrections were used only for the vibration–rotation constants, Eq. (7), but not for the spin–spin and spin–rotation constants, Eqs. (8) and (9). The standard error of these fits was 4.5, so this model does not provide an adequate description of the spectroscopic data. It was necessary to add Born–Oppenheimer breakdown correction terms to some of the spin–spin and spin–rotation constants to fit all of the data.

The obtained Dunham constants of the $X^3\Sigma^-$, $a^1\Delta$, and $b^1\Sigma^+$ electronic states of four isotopologues of SbH are displayed in Tables 6 and 7. The number of significant digits of these constants was minimized by the procedure of sequential rounding and refitting [23] incorporated into the DPARFIT program. In our fit, the observed data can be reproduced to within 1.1 times their respective uncertainties. The T_e values for each isotopologue of Table 7 are relative to the $v'' = -1/2$ level of the ground $X^3\Sigma^-$ state. In general, the magnitude of Born–Oppenheimer breakdown correction terms is small. However, the correction to γ_D is larger than γ_D itself, and thus, the γ expansion parameters should be treated as effective parameters.

In conclusion, our work has resulted in a substantial improvement in the spectroscopic constants of SbD and, particularly, SbH for the $X^3\Sigma^-$, $a^1\Delta$, and $b^1\Sigma^+$ states. Our new constants are both more extensive and more precise than the previous work. In addition, we also found that Born–Oppenheimer breakdown corrections are also needed for the spin–spin and spin–rotation interaction terms. We did not see the SbH_2 or SbH_3 molecules in our spectra.

Acknowledgments

Funding for this work was provided by the Natural Sciences and Engineering Research Council (NSERC)

of Canada. We thank E.H. Fink for sending us the unpublished line positions of the 1–1 bands of the $a^1\Delta$–$X^3\Sigma^-$ transitions of SbH and SbD. We would also like to thank Professor Robert J. Le Roy for discussions and for help with the combined-isotopologue fit.

Appendix A. Supplementary data

Supplementary data for this article are available on ScienceDirect (www.sciencedirect.com) and as part of the Ohio State University Molecular Spectroscopy Archives (http://msa.lib.ohio-state.edu/jmsa_hp.htm).

References

[1] P. Bollmark, B. Lindgren, Chem. Phys. Lett. 1 (1967) 480.
[2] N. Basco, K.K. Yee, Spectrosc. Lett. 1 (1968) 13–15.
[3] P. Bollmark, B. Lindgren, Phys. Scripta. 10 (1974) 325–330.
[4] P. Bollmark, B. Lindgren, U. Sassenberg, Phys. Scripta. 24 (1981) 542–550.
[5] V. Stackmann, K. Lipus, W. Urban, Mol. Phys. 80 (1993) 635–645.
[6] R.-D. Urban, K. Essig, H. Jones, J. Chem. Phys. 99 (1993) 1591–1596.
[7] M. Beutel, K.D. Setzer, O. Shestakov, E.H. Fink, J. Mol. Spectrosc. 179 (1996) 79–84.
[8] O. Shestakov, R. Gielen, A.M. Pravilov, K.D. Setzer, E.H. Fink, J. Mol. Spectrosc. 191 (1998) 199–205.
[9] X. Wang, P.F. Souter, L. Andrews, J. Phys. Chem. A 107 (2003) 4244–4249.
[10] K. Balasubramanian, N. Tanpipat, J.E. Bloor, J. Mol. Spectrosc. 124 (1987) 458–463.
[11] A.B. Alekseyev, H.-P. Liebermann, R.M. Lingott, O. Bludsky, R.J. Buenker, J. Chem. Phys. 108 (1998) 7695–7706.
[12] S. Hirata, T. Yanai, W.A. de Jong, T. Nakajima, K. Hirao, J. Chem. Phys. 120 (2004) 3297–3310.
[13] A. Shayesteh, K. Tereszchuk, P.F. Bernath, R. Colin, J. Chem. Phys. 118 (2003) 1158–1161.
[14] A. Shayesteh, D.R.T. Appadoo, I.E. Gordon, R.J. Le Roy, P.F. Bernath, J. Chem. Phys. 120 (2004) 10002–10008.
[15] A. Shayesteh, K. Tereszchuk, P.F. Bernath, R. Colin, J. Chem. Phys. 118 (2003) 3622–3627.
[16] A. Shayesteh, D.R.T. Appadoo, I. Gordon, P.F. Bernath, J. Chem. Phys. 119 (2003) 7785–7788.
[17] B. Edlen, Metrologia 2 (1966) 71–80.
[18] W. Whaling, W.H.C. Anderson, M.T. Carle, J.W. Brault, H.A. Zarem, J. Res. Natl. Inst. Stand. Technol. 107 (2002) 149–169.
[19] G. Herzberg, Molecular Spectra and Molecular Structure. δ. Spectra of Diatomic Molecules, Van Nostrand, Princeton, NJ, 1950.
[20] C.R. Brazier, R.S. Ram, P.F. Bernath, J. Mol. Spectrosc. 120 (1986) 381–402.
[21] R.J. Le Roy, J. Mol. Spectrosc. 194 (1999) 189–196.
[22] R.J. Le Roy, "DParFit 3.0. A Computer Program for Fitting Diatomic Molecular Spectral Data to Parameterized Level Energy Expressions", University of Waterloo, Chemical Physics Research Report CP-658 (2004). Available from: <http://scienide.uwaterloo.ca/~leroy/dparfit>.
[23] R.J. Le Roy, J. Mol. Spectrosc. 191 (1998) 223–231.